

DESIGN AND OPTIMIZATION OF UNDERTRAY FOR FORMULA SAE  
RACE CAR USING CFD ANALYSIS

by

GIRISH BANGALORE JALAPPA

Presented to the Faculty of the Graduate School of  
The University of Texas at Arlington in Partial Fulfillment  
of the Requirements  
for the Degree of  
MASTER OF SCIENCE IN MECHANICAL ENGINEERING

THE UNIVERSITY OF TEXAS AT ARLINGTON

AUGUST 2015

Copyright © by GIRISH BANGALORE JALAPPA 2015

All Rights Reserved



## Acknowledgements

I am grateful to my parents Jalappa and Sheela, who have worked hard to provide myself and my sister with a good, strong education. They are the reason that I became an engineer.

I would also like to thank my advisor Dr Robert Woods, who has been an exceptional advisor and mentor.

I would specifically like to thank my teammates James Merkel and Michael Rex who have worked with me on the aerodynamics systems of the FSAE cars and all the UTA FSAE Racing team members who I worked with for last two and a half years.

March 5, 2015

## Abstract

# DESIGN AND OPTIMIZATION OF AN UNDERTRAY FOR FORMULA SAE RACE CAR USING CFD ANALYSIS

Girish Bangalore Jalappa, MS

The University of Texas at Arlington, 2015

Supervising Professor: Robert L. Woods

With the advent of inverted wings to produce down-force in Formula-1 during the 1960's, aerodynamics has played a big role in increasing the vehicle performance. An aerodynamics system consists of front, rear wings and an under-tray. This thesis focuses on design of a new under-tray using CFD analysis for a Formula-SAE car.

## Table of Contents

Acknowledgements .....	iii
Abstract .....	iv
List of Illustrations.....	vii
List of Tables .....	x
Chapter 1 Introduction.....	1
1.1 Vehicle Aerodynamics.....	2
1.2 Aerodynamics .....	3
1.3 Under-tray .....	4
Chapter 2 Two Dimensional Inlet Angle Analysis.....	6
2.1 Overview .....	6
2.2 2-D Model Considerations.....	7
2.3 Limitations .....	10
2.4 Results .....	11
Chapter 3 Three Dimensional Analysis .....	13
3.1 Mesh sizing study for 3-D Analysis .....	16
3.2 Limitations and Bench Marking .....	19
3.3 3D Diffuser Angle study .....	20
3.3.1 Overview.....	20
3.3.2 Results.....	21
3.4 3-D Inlet and Diffuser Radius Study .....	25

3.5	Use of Curvature combs for diffuser tunnel .....	27
3.6	Additional Second Diffuser .....	29
3.6.1	Overview.....	29
3.6.2	Results.....	31
3.7	3-D Gurney Flap Study .....	31
3.7.1	Overview.....	31
3.7.2	Result .....	33
3.8	3-D Analysis Of Final Model.....	35
3.8.1	Results.....	42
3.9	Ride Height Study .....	43
3.10	Recommendations .....	45
	References .....	46
	Biographical Information.....	47

## List of Illustrations

Figure 1: Fluid flow over airfoil.....	3
Figure 2: Illustration of a vehicle in ground effect .....	4
Figure 3: Baseline Under-tray Cross Section.....	5
Figure 4 : Two Dimensional point-wise model .....	8
Figure 5: Figure of velocity vector plot.....	10
Figure 6: Velocity vector plot with diffuser separation.....	11
Figure 7: Inlet angle study .....	12
Figure 8: Inlet area ratio study .....	12
Figure 9: Solid Works model with extra piece on the bottom of diffuser to stop flow diffusion through the tire cut part .....	14
Figure 10: Solid works mode of a splitter in the diffuser to stop flow diffusion .....	14
Figure 11: Solid works of a diffuser with horizontal and vertical opening to improve diffusion rate .....	14
Figure 12: Solid works model tried to divert the flow away from the tire cut.....	15
Figure 13: Three dimensional mesh study.....	17
Figure 14: Three Dimensional Point-wise mesh Generation .....	18
Figure 15: Three Dimensional Under-tray with mesh .....	18

Figure 16: Solid works model of three dimensional half under-tray with single diffuser used for analysis.....	21
Figure 17: Pressure Coefficient plot straight diffuser .....	22
Figure 18: Pressure Coefficient plot straight diffuser with tire cut.....	22
Figure 19: Diffuser angle study for straight throat.....	23
Figure 20 : Pressure Coefficient plot of Curved diffuser .....	24
Figure 21: Pressure Coefficient plot for curved diffuser with tire cut.....	24
Figure 22: Diffuser angle study for curved throat.....	25
Figure 23: Inlet Radius study.....	26
Figure 24: Diffuser radius study.....	26
Figure 25: Curvature combs for old under-tray .....	28
Figure 26: Curvature combs for new under-tray design.....	28
Figure 27: Solid works model of under-tray with double diffusers.....	29
Figure 28: Solid works model of under-tray with double diffusers.....	30
Figure 29: Cp for under-tray Double Diffusers .....	31
Figure 30: Solid works model of double diffuser under-tray with gurney .	32
Figure 31 : Pressure Coefficient plot for double diffuser with gurney flap.....	34
Figure 32: Pressure Coefficient plot for double diffusers with gurney flap.....	34
Figure 33 : Velocity stream lines for double diffusers with gurney flap ....	35



Figure 34 : Solid works full under-tray model.....	36
Figure 35: Solid works full under-tray model with tires .....	36
Figure 36 : Pressure Coefficient plot for under-tray with tires-1 .....	37
Figure 37: Pressure Coefficient plot for under-tray with tires-2.....	37
Figure 38 : Velocity streamlines for Under-tray with tires .....	38
Figure 39: Velocity stream lines for double diffusers with gurney flap .....	38
Figure 40: Pressure curves from inlet to diffuser outlet .....	39
Figure 41: Pressure Coefficient vs Length of under-tray (First Diffuser)..	40
Figure 42: Pressure Coefficient vs Length of under-tray (Second Diffuser) .....	40
Figure 43 : Pressure coefficient plot of Under-tray With 2-Degree Pitch .	41
Figure 44: Pressure Coefficient vs Length of under-tray .....	41
Figure 45:Pressure Coefficient at 1.5in ride height.....	43
Figure 46:Figure 45:Pressure Coefficient at 1in ride height.....	44

## List of Tables

Table 1: Grid independence study Ride height=1.75in (44.45mm).....	9
Table 2: Diffuser study for second diffuser .....	30
Table 3: Gurney flap study for under-tray with double diffuser .....	33
Table 4: Final results of 3-D analysis.....	42

## Chapter 1

### Introduction

Formula SAE is collegiate design competition organized by Society of Automotive Engineers (SAE) to give students hands on experience to design, build and test/race an open wheeled Formula type car. It was started in the year 1981, University of Texas Arlington are one of the 4 founding teams of the competition.

Each year a set of rules are given to design a Formula type race car. The car is judged on static and dynamic events. In static events, cars are judged on the design, cost analysis of the car, business and marketing presentation. Dynamic events include drag race to test acceleration potential of the car, skid pad to test the handling, autocross to test the ability of the car to maneuver around the course and a endurance event to test if the car can last for a particular distance.

## 1.1 Vehicle Aerodynamics

"In a car, driving, braking and cornering forces are created at the contact patch between the tire and the road. These friction-like forces are strongly affected by the vertical force applied on the tires and are limited by some maximum friction coefficient." (1)

"Now, if we could increase the normal tire force by pushing the tire more against the road, then the cornering force could be increased, too, without the risk of sliding. One way to do this is to add more weight to the car. But this won't work because an increase in the car's mass will affect the lateral acceleration at the same rate. Therefore there will be no improvement in the turn rate, and even worse, the car will be heavier." (1)

"Aerodynamic down force increases loads on the tires without increasing the vehicles weight. The result is increased cornering ability with no weight penalty, which gives a reduction in lap times." (1)

## 1.2 Aerodynamics

Aerodynamics is the study of motion of air around an object or in this case a vehicle. We are concerned with calculation of forces on and around an object. The forces that interests us for this paper are lift and drag.

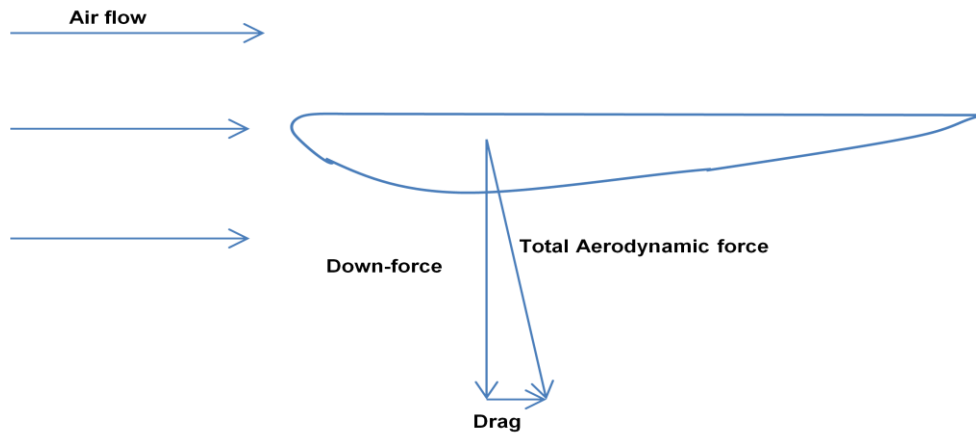


Figure 1: Fluid flow over airfoil

Air flowing over an airfoil travels at different velocities above and below the airfoil due to its shape. From Bernoulli's principle we know that as the velocity increases the pressure decreases and vice versa. Due to the difference in pressures a force is generated. This force is directed towards the suction or low pressure side of the airfoil. In race Car aerodynamics we call it down-force. Drag force is the force generated in the opposite direction of motion of an object, when it moves through a fluid.

### 1.3 Under-tray

An Under-tray is a down-force producing device. The force generated is amplified by utilizing its proximity to the (This is called ground effect). The underside of the under-tray is designed like the shape of bottom of an airfoil. The Figure 2 below shows under side of a car designed like bottom part of the wing, the air is accelerated by creating a nozzle effect at the inlet. Figure 3 shows a two dimensional undertray tunnel with all the different parts.

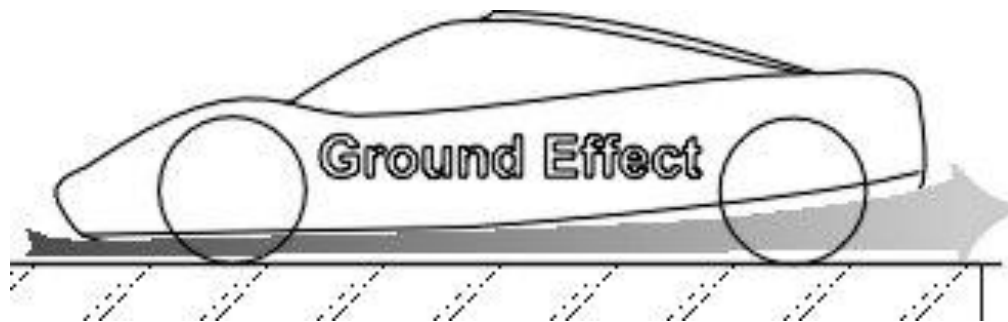


Figure 2: Illustration of a vehicle in ground effect

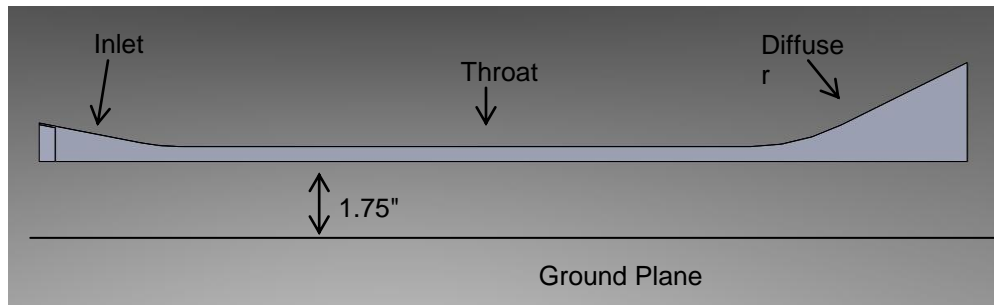


Figure 3: Baseline Under-tray Cross Section

## Chapter 2

### Two Dimensional Inlet Angle Analysis

#### 2.1 Overview

The objective of this study was to look at how changing the inlet area ratio would influence the  $C_i$ . The inlet area ratio is the ratio of the height of the inlet divided by the height of the throat section. Figure 4 illustrates the figure of a unit span profile of an under-tray.

Figure 6 shows a velocity contour plot of a typical 2D simulation. There is a flow separation along the diffuser wall as the air exits the throat region. Usually air from the sides of the under tray is sucked into the straight and lateral flow creates vortices in the diffuser section. These vortices energize the flow and help them stay attached at higher diffuser angles. The flow should be attached along the inlet, throat and throughout the diffuser. Hence the 2-D study was used for inlet area ratio study only. In the 2-D study, we are looking for trends in  $C_i$  caused by inlet area ratio and not actual numbers. Inlet was studied in two different methods. The first method was the inlet angle study where inlet angle was changed with no change in the length of the inlet. The angles looked at were  $3^\circ$ ,  $6^\circ$ ,  $9^\circ$ ,



12°, and 15°. The second method kept the inlet angle fixed while the inlet length was varied.

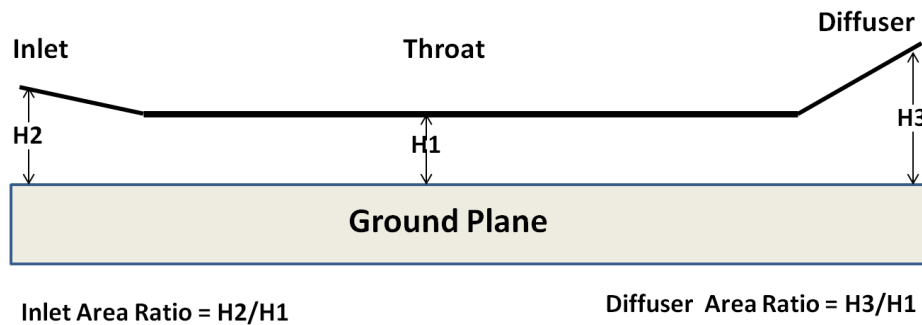


Figure 4: Area ratio schematic

## 2.2 2-D Model Considerations

The 2D study was done entirely in Star Ccm+ version9. The profiles of 2-D models were exported from solid works into point-wise, in igs format. The model was meshed in point- wise before it was exported to Star Ccm+ for analysis. "All the other geometry like suspension arms, front wing and chassis was neglected for the 2-D study" (2). This kept the complexity of the model and computational time of each simulation to a minimum. All the 2-D models were run at three different velocities 15 m/s (33.5 mph), 22.5 m/s (50 mph) and 30 m/s (67 mph). The objective was to identify how every setup performed at speeds typical to speeds of a Formula SAE competition. Each case was run at the 1.75 inch ride height. To ensure

that the results were not adversely affected by boundary layer growth a moving ground plane was used. Since the under tray was modeled in ground effect the turbulence was modeled using the K - epsilon model. The figure below illustrates a typical 2D model. The size of the domain was a 5X times size in front, 10X times the size behind the model and 5X times the height to imitate a wind tunnel.

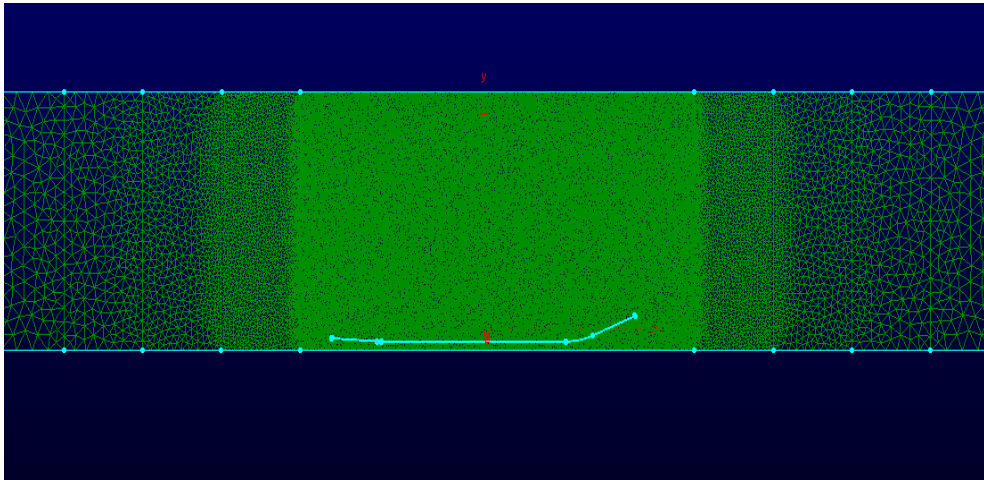


Figure 4 : Two Dimensional point-wise model

A triangular unstructured mesh was chosen due to the ease in creating 2D meshes around irregularly shaped structures. The sizes of the elements along the 2D cross section were controlled using sizing functions. The mesh size was gradually increased from 0.3 to 2 (non-dimensional) to reduce the computation time. The mesh was generated away from the 2D cross section till the boundaries of the control surface. A grid

independence study was conducted to find the sizing function that would yield acceptable results and converge to a solution rapidly. Several different size functions were looked at before choosing a cell size of 0.3, a growth decay of 0.9, and a final cell size of 2. Table-1 shows a comparison between five meshes over a similar inlet configuration at a ride height of 1.75 inches.

Table 1: Grid independence study Ride height=1.75in (44.45mm)

Mesh	Number of Iterations to converge	Time Taken for Convergence(min)	$C_d$	$C_l$
0.5	1700	8	1.7	0.6673
0.3	3000	20	1.7	0.6458
0.1	3300	45	1.7	0.6458
0.05	3650	85	1.7	0.6458

## 2.3 Limitations

Before the results are presented, it is important to understand about the limitations of the 2-D study. The 2-D studies are concerned only with how changing the inlet area ratio affects the throat and the diffuser inlet section. These studies have focused on trends and not absolute numbers. As stated previously, it became apparent early on that an under-tray could not be fully analyzed with a 2D model. The effects of the air coming in from the sides of the under tray and creating vortices within the tunnels could not be captured. Thus trying to get a benchmark these models is nearly an impossible task. The following velocity contour plot figure 6 and the velocity vector plot figure 7 show the separation at diffuser angle of  $20^\circ$  as discussed in above section 2.1.

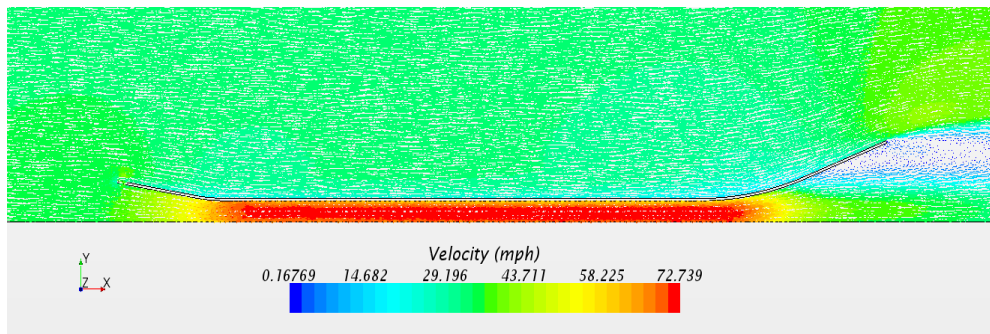


Figure 5: Figure of velocity vector plot

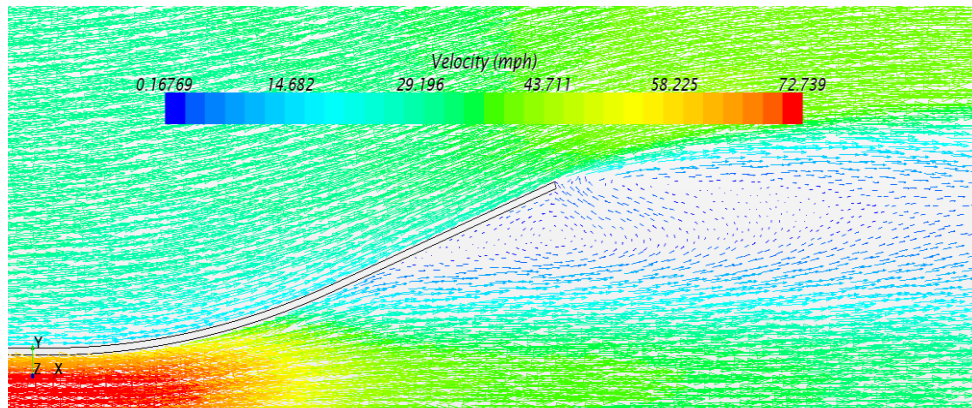


Figure 6: Velocity vector plot with diffuser separation

## 2.4 Results

The average lift of each configuration was the sum of the total lift for each velocity divided by three. The average lift of each of these models increased with the increase in area ratio and inlet angle. Using the average lift provided a picture of how each configuration performed over the range of velocities typical in a SAE competition. Finally, the lift numbers for the inlet ratio studies reflect the lift of a 2D cross section and not of the entire under tray.

In the varied inlet angle approach the area ratios were varied from 1.25 to 2.25. In this study the  $C_l$  varied from 2.98 to 3.25. The baseline configuration an inlet angle of  $3^\circ$  showed a  $C_l$  of 3.04. Thus, increasing the inlet angle to  $9^\circ$  increased the  $C_l$  of the 2D cross section by 8% to

3.28. The figure 9 below illustrates this study. Figure 9 illustrates inlet area ratio study, area ratio of 1.9 was selected which has a  $C_l$  of 3.3.

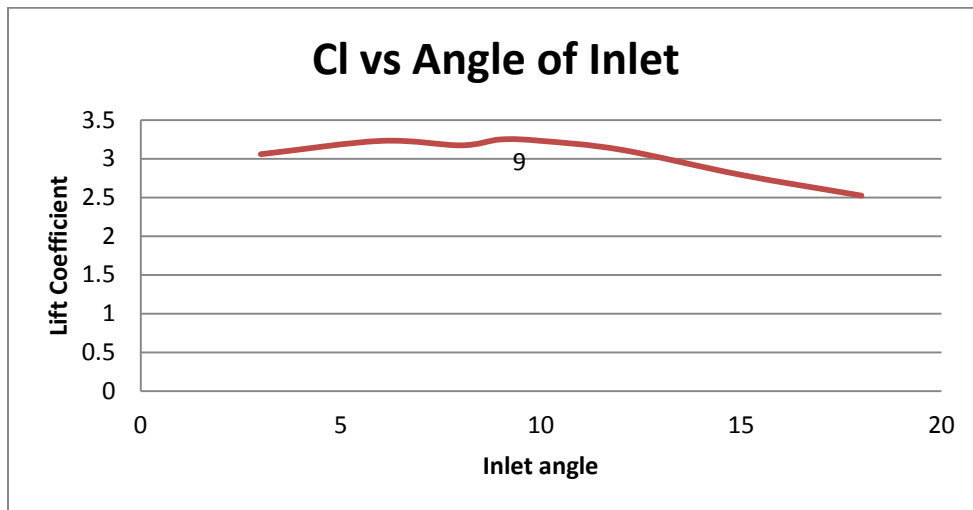


Figure 7: Inlet angle study

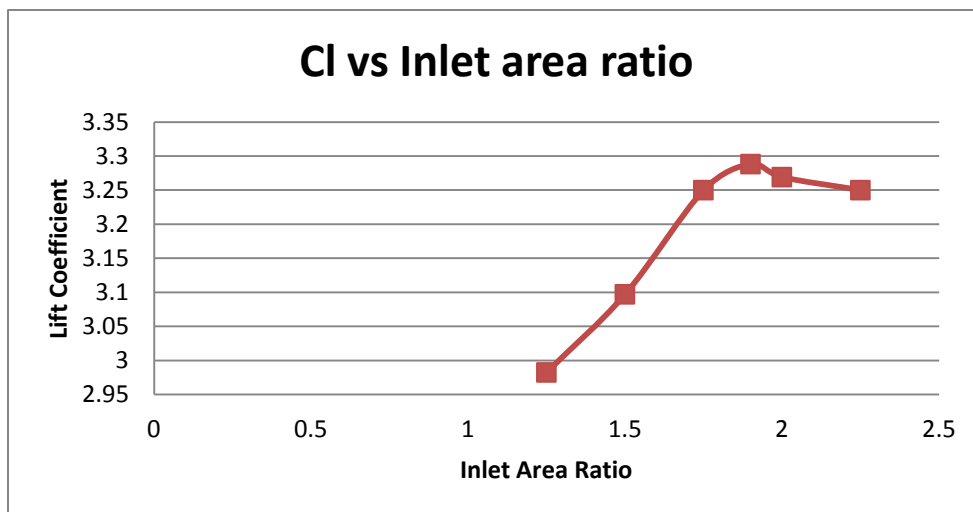


Figure 8: Inlet area ratio study

## Chapter 3

### Three Dimensional Analysis

The concepts modeled and tested to increase the down force are diffuser area ratio on the base model, model with a tire cut on the under tray to package the model, adding tires to the model to discover effects of a rotating tire, additional second diffuser and addition of a gurney flap. These modifications are addition to the base model geometry of the under tray. These models are tested in star ccm+ to accurately simulate the flow field around the under tray. The 3D analysis is able to simulate the air being sucked into from the sides of the under-tray which creates vortices that help to stay attached in at higher angles in the diffuser section, which is not possible in 2-D analysis. From 3-D analysis it is possible to predict actual lift numbers. All the models were run at velocities ranging from 15m/s (33.5mph), 22.5m/s (50mph), 30m/s (67mph) to simulate velocities that are seen in a Formula SAE competition. Studying previous studies and papers on under-tray helped us to come to this conclusion to use the splitter and a wider inlet depending on packaging area available as in reference (2). Figure11-14 show various diffuser styles tested to improve  $C_i$ .

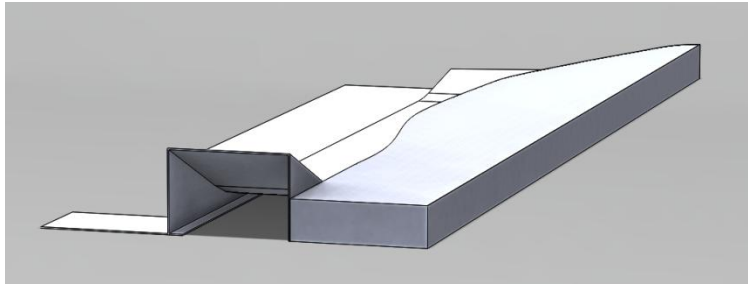


Figure 9: Solid Works model with extra piece on the bottom of diffuser to stop flow diffusion through the tire cut part

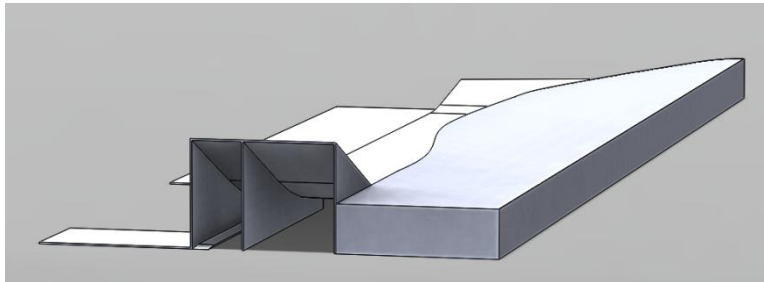


Figure 10: Solid works mode of a splitter in the diffuser to stop flow diffusion

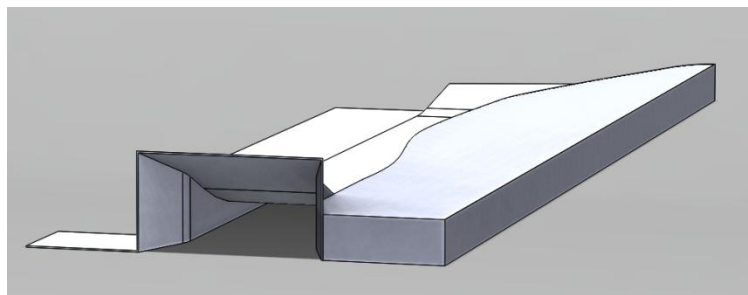


Figure 11: Solid works of a diffuser with horizontal and vertical opening to improve diffusion rate



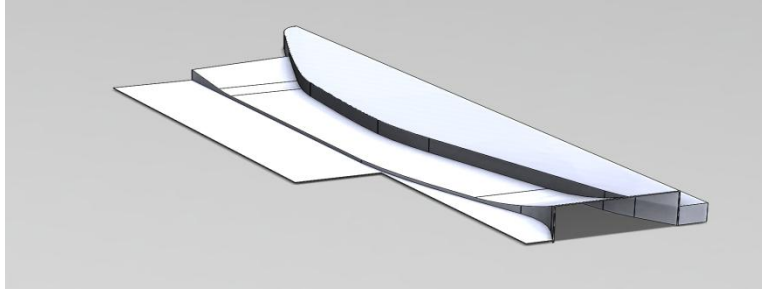


Figure 12: Solid works model tried to divert the flow away from the tire cut

Each configuration was modeled in solid-works and the geometry was exported in iges format. The iges file was imported to point-wise to create the required mesh. The control volume for the mesh is 5X times the size of the model in front of it, 10X times the size of the model behind it, 5X times size of the model in width and 5X times size of the model in height. The current base model is 78in in length and 52in in width. In order to save computation time half of the under-tray was modeled and a symmetry wall was used. Also some parts like suspension geometry, front wing and chassis were neglected for most of the study to reduce the number of tetrahedron elements to around 9 million cells for just the under-tray and around 15 million cells with the tires. All the edge of the under tray was meshed individually. From there face meshes were created and evaluated. The meshes created were well below 0.85 with regard to equi angle skew and equi-size skew. Thus, when the volume was meshed the

result would be a mesh with very few elements that approach the 0.85. Limit. All the models were run on an 8 core processor workstation with 10GB of RAM in the FSAE Design Lab. Time for convergence averaged around 8hrs for models just with the under-tray and 12 hrs for models with under -tray and tires. K-epsilon turbulence model was used to simulate flow characteristics of the turbulent flow. The residuals used to determine convergence were continuity, turbulent kinetic energy “k”, and the dissipation rate of turbulent kinetic energy “ $\epsilon$ ”. All of the residuals were set to .001. It is one of the most commonly used turbulence models for CFD. The K-epsilon model has a good balance between amount of time taken to converge and accuracy. Since we are running many models K-epsilon was chosen. The following figure illustrates a 3-D point-wise model.

### 3.1 Mesh sizing study for 3-D Analysis

Same procedure followed for 2-D is followed for 3-D mesh study. For 3-D mesh study a single 3-D model is run with different mesh sizes. After running all the considered mesh sizes we look for time taken for convergence and accuracy of a result. Depending on accuracy, time taken and the computational power available, we decide upon a single mesh size for all of our 3-D analysis. So that the results from the 3-D simulations are independent of mesh size. A non-dimensional mesh size of 0.3 was

used. Figure-16, 17 below shows the mesh generated for the studies. Figure-15 illustrates three dimensional mesh study.

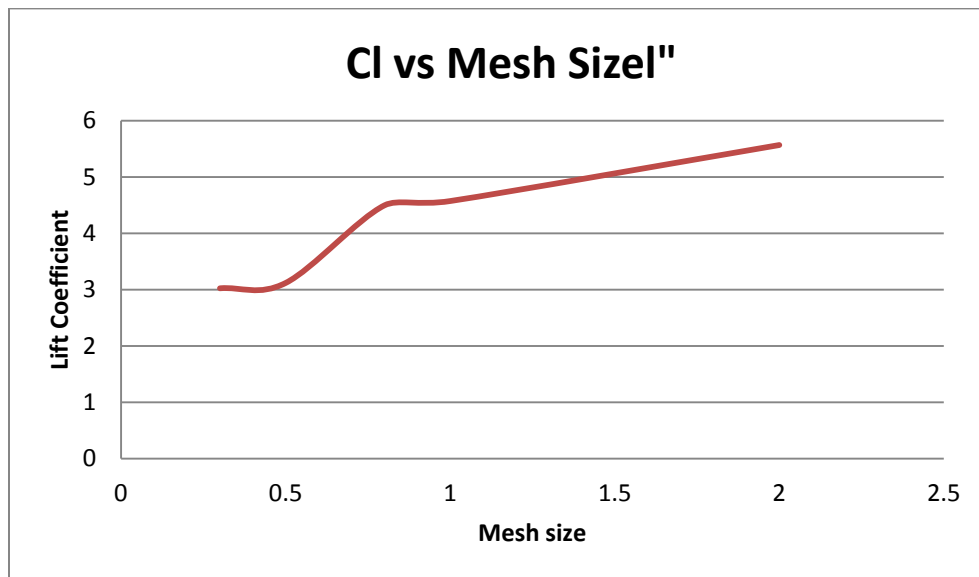


Figure 13: Three dimensional mesh study

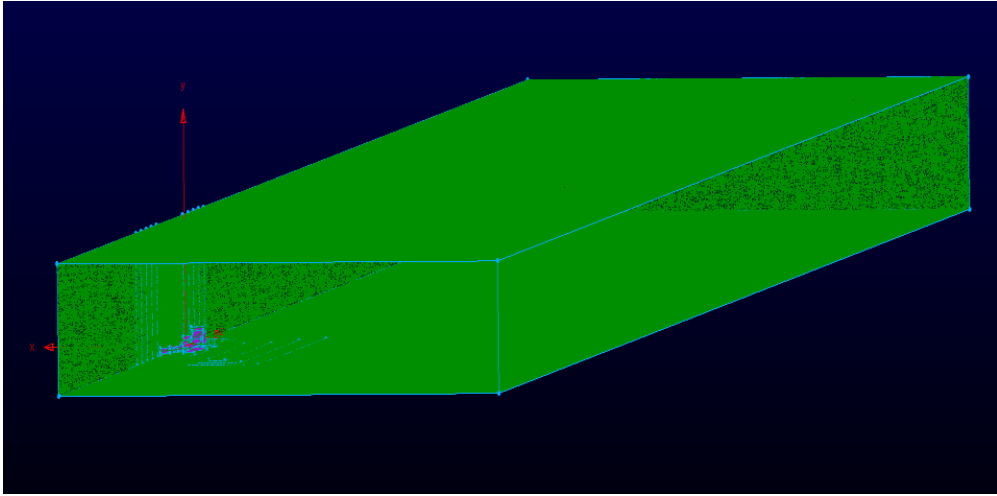


Figure 14: Three Dimensional Point-wise mesh Generation

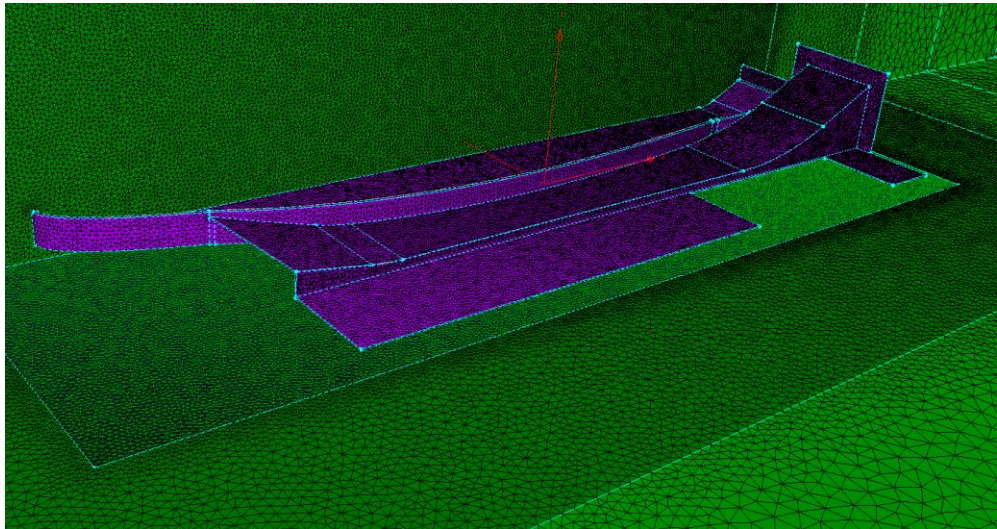


Figure 15: Three Dimensional Under-tray with mesh

### 3.2 Limitations and Bench Marking

We don't have wind tunnel access to correlate with the CFD data. We made attempts to measure the deflection of the suspension and back calculate the lift numbers the wings and under tray were producing, but that data was deemed unreliable because of false measurements and lack of a good data acquisition system. This has left us with CFD analysis done in 2006 as the primary source of information for correlation of 3-D models. The 2006 analysis was validated by a professional CFD company Power flow. As mentioned before the under-tray was the only model meshed for initial diffuser area ratio and diffuser angle study, since the diffuser sees clean air and the computational time can be saved. Later we added tires to investigate the effects of tires to the diffuser section. This saved us time and allowed us to try many more models since just one model had to be re-meshed. In order to correlate the CFD study with previous CFD data we ran a simulation of the old under-tray design. The numbers were similar to the analysis done in 2006. This gave us a good idea what our previous under-tray numbers were and it was easy to compare.

### 3.3 3D Diffuser Angle study

#### 3.3.1 Overview

The diffuser angle study is similar to the inlet angle study used in the 2D inlet study. The angle of the diffuser was modified by moving the rear edge of the diffuser up or down. The diffuser in the baseline under tray (diffuser used in inlet study) has a 20° exhaust angle. The angles which were studied were 18°, 20°, 22°, 24°, and 26°. The reduced angles of 18° and 20° were looked at to make sure that the baseline configuration had not been designed with too aggressively. Since the width of the tunnels remained a constant during the study. For the 3D analysis the surfaces of the under tray were subdivided into the areas shown in the following figure. For each run the lift for each section was recorded and compared to the baseline configuration.

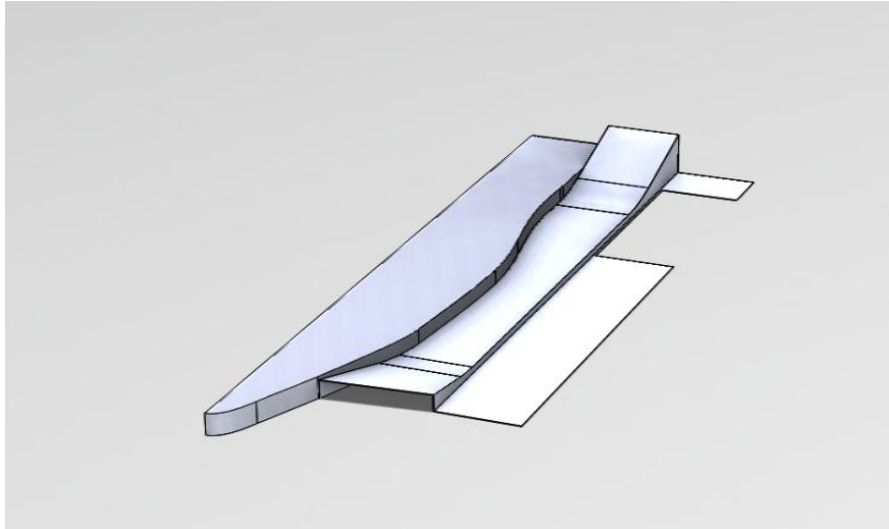


Figure 16: Solid works model of three dimensional half under-tray with single diffuser used for analysis

### 3.3.2 Results

The results showed us that as the diffuser angle increased the lift also increased. There was no separation in the diffuser walls until diffuser angle reached 26 degree. Angles more than 26 degree were not tested since they could not be packaged due to the suspension and chassis package. There was no reduction in lift indicating any separation within the diffuser walls. The average  $C_L$  for the 18° case was 0.42 and 0.28 for straight and curved diffuser respectively, while the average  $C_L$  for the 18°

with tire cut was 0.21 and 0.12 for the under-tray with tire cut case. Thus there is a 50% or more loss with the tire cut models.

. Figures 24 and 27 illustrate how increasing the rear angle affects the entire under tray for both straight and curved diffuser tunnels.

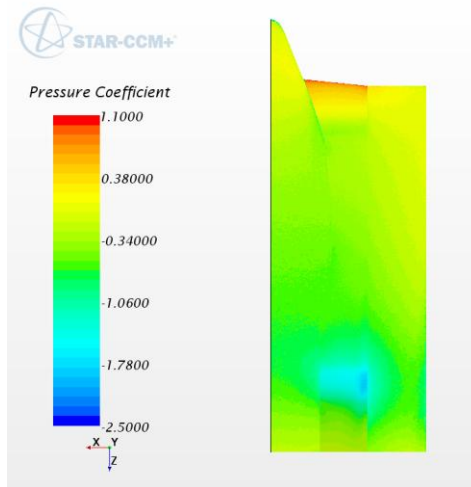


Figure 17: Pressure Coefficient plot straight diffuser

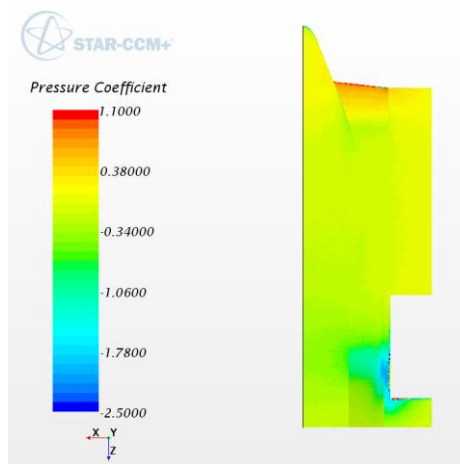


Figure 18: Pressure Coefficient plot straight diffuser with tire cut



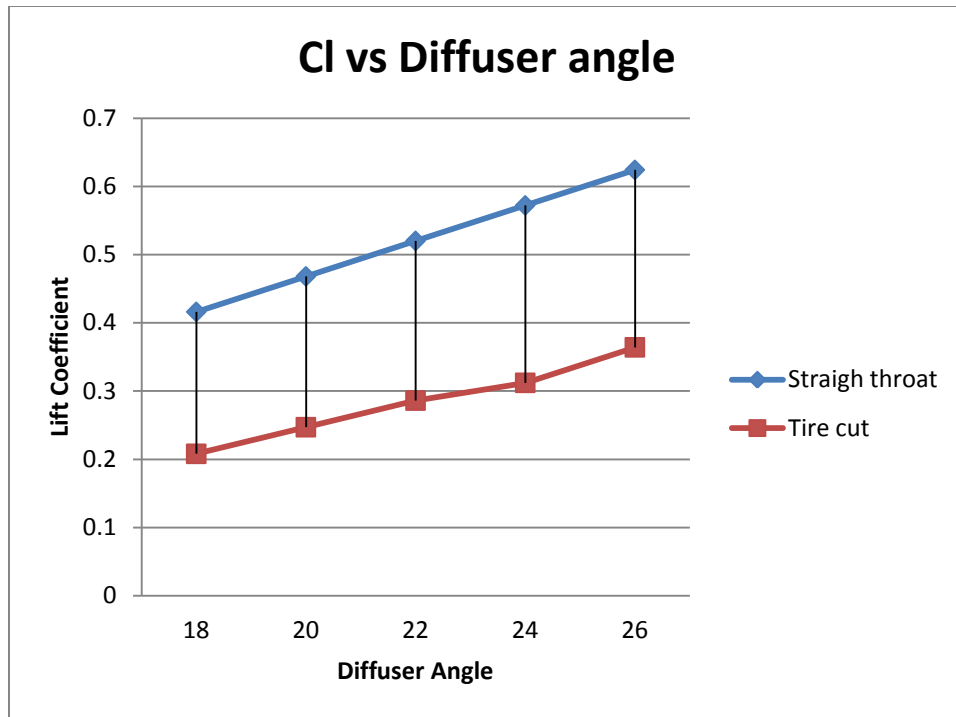


Figure 19: Diffuser angle study for straight throat

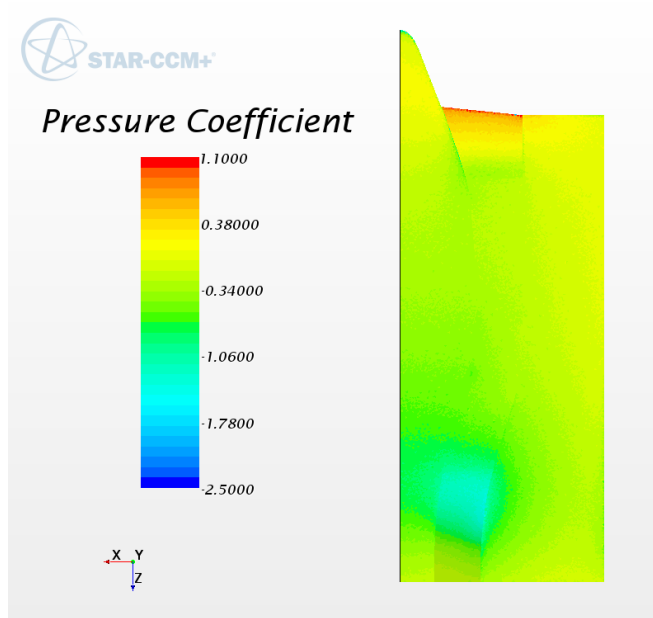


Figure 20 : Pressure Coefficient plot of Curved diffuser

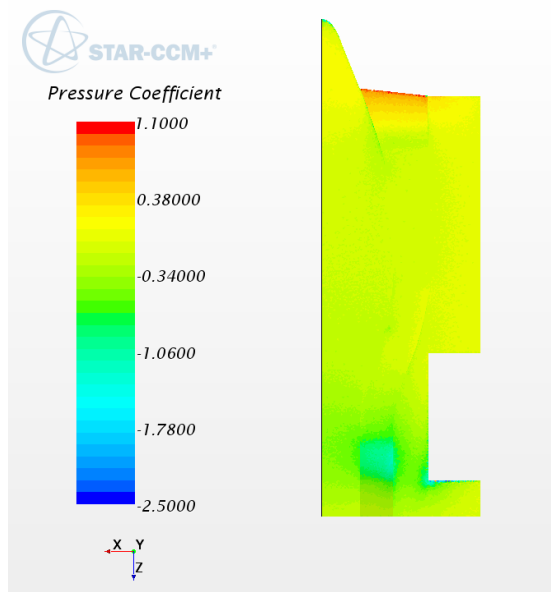


Figure 21: Pressure Coefficient plot for curved diffuser with tire cut

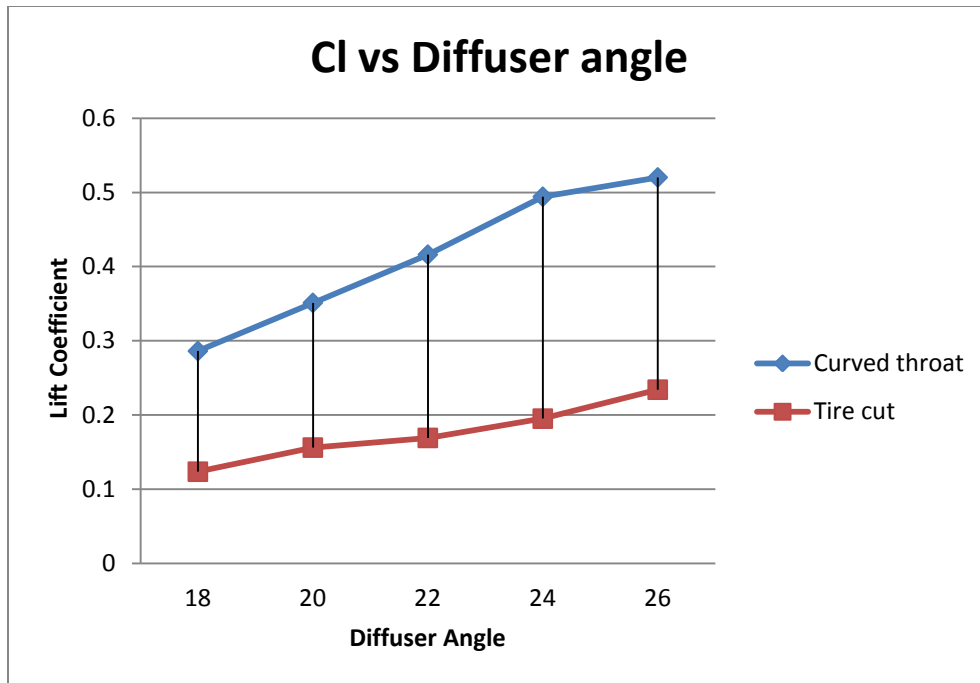


Figure 22: Diffuser angle study for curved throat

### 3.4 3-D Inlet and Diffuser Radius Study

After the inlet and the diffuser angles were studied, an inlet and diffuser angle study was performed. For this study a constant inlet angle of 9 degree and constant diffuser angle of 26 degree was used.

Four different radius for both inlet and diffuser was tested. For the inlet the radius tested were 15in, 20in, 25in, and 30in at inlet and diffuser angle of 9 °and 20° respectively. The diffuser radius tested were 10in, 20in, 30in, and 40in at inlet and diffuser angle of 9° and 26° respectively. The values

of radius tested depending on packaging capacity. For both the inlet and outlet we ended up using 30in of radius.

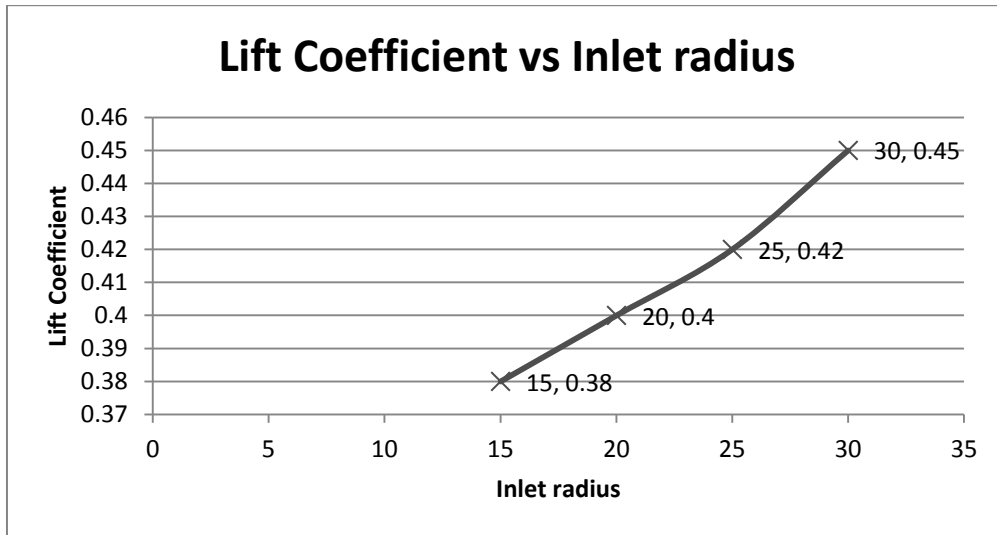


Figure 23: Inlet Radius study

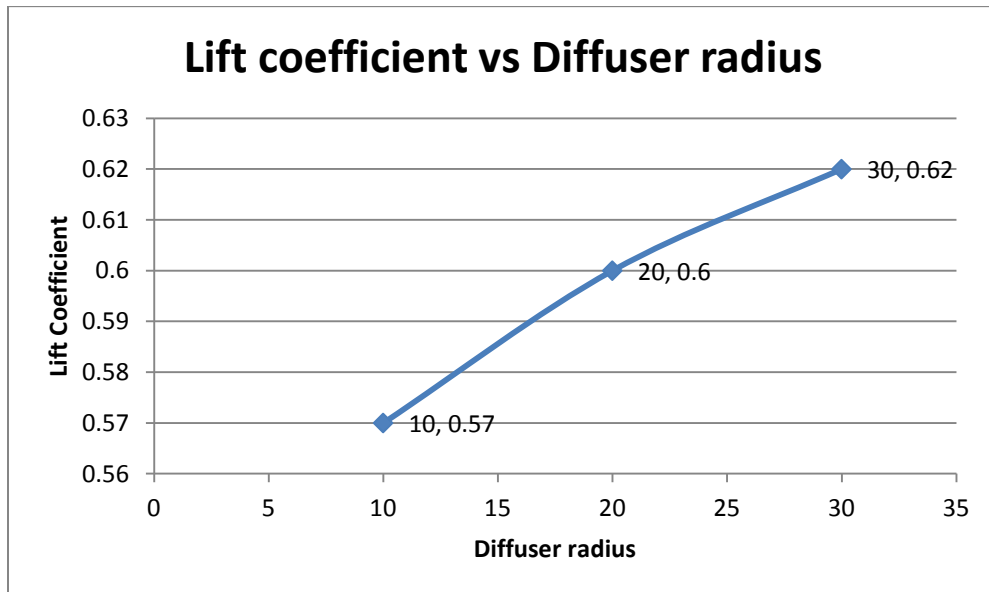


Figure 24: Diffuser radius study

### 3.5 Use of Curvature combs for diffuser tunnel

The underside of the under-tray is designed to mimic a lower side of the airfoil. The design of the underside is sensitive to pressure changes. Going one step ahead the sides of the tunnel from the inlet till the diffuser inlet is shaped like the underside of the airfoil.

Curvature combs helps us by providing an enhancement of the slope and curvature in the sketch.

With the use of curvature combs from solid works the smallest variation in drawing can be controlled which in turn controls the pressure gradient. As can be seen in the below figure-30 the sides of tunnels from 2006 under-tray and present under-tray in figure-31. The curvature combs shows a smoother and reducing pressure gradient rather than the varying gradient on the old under-tray design.

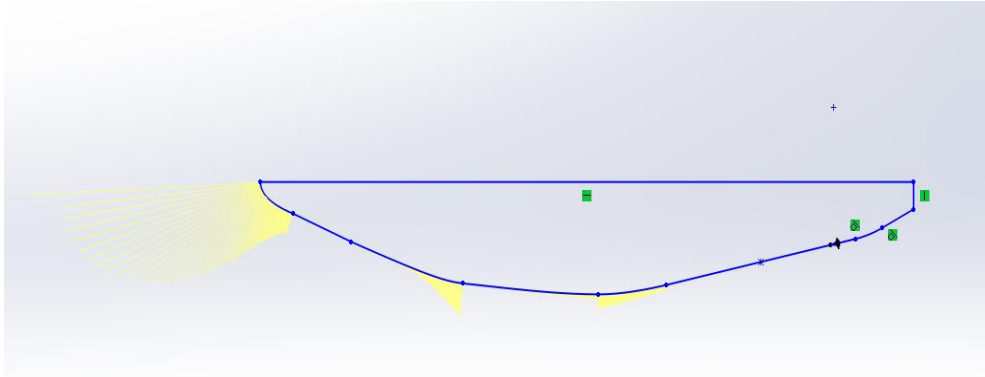


Figure 25: Curvature combs for old under-tray

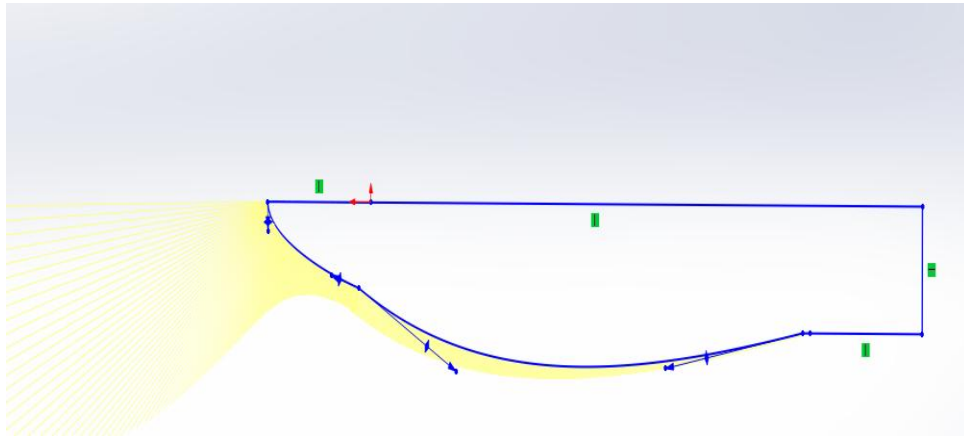


Figure 26: Curvature combs for new under-tray design

## 3.6 Additional Second Diffuser

### 3.6.1 Overview

One of the concepts that was modeled in solid-works was the additional second diffusers next to the big diffusers. Because of packaging the second diffuser is only 6 inches long. There was extra room after the chassis to package this second diffuser. In the case of the second diffuser the various angles were tested from 18°-26°. Table-2 shows us how the second diffuser improves the  $C_i$ . A radius of 3in between diffuser and throat was selected. The figures-32, 33 below shows the under-tray with double diffusers as modeled in solid-works. The second diffuser added around million cells to the model to make it total of 9 million cells

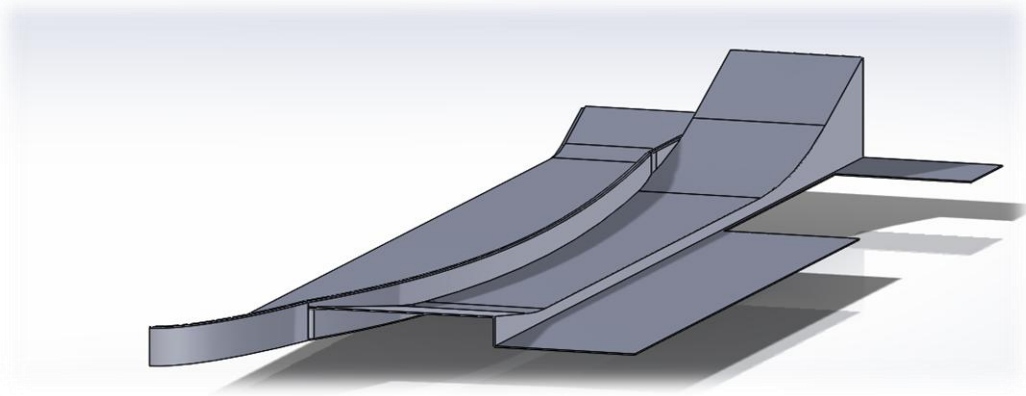


Figure 27: Solid works model of under-tray with double diffusers

Table 2: Diffuser study for second diffuser

D1(Angle)	D2(Angle)	Down-force	Cl
26	26	31	.40
26	24	28	.36
26	22	27	.35
26	20	25	.33
26	18	22	.29

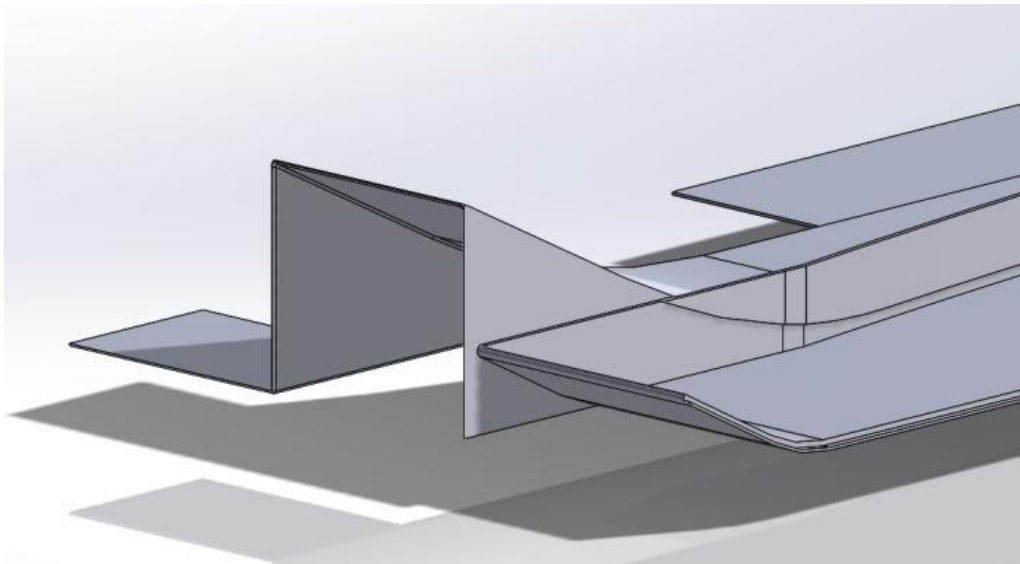


Figure 28: Solid works model of under-tray with double diffusers



### 3.6.2 Results

The addition of the second diffuser increases the  $C_l$  of the under tray from 0.36 to 0.4. This is an increase of 11% in the  $C_l$ .

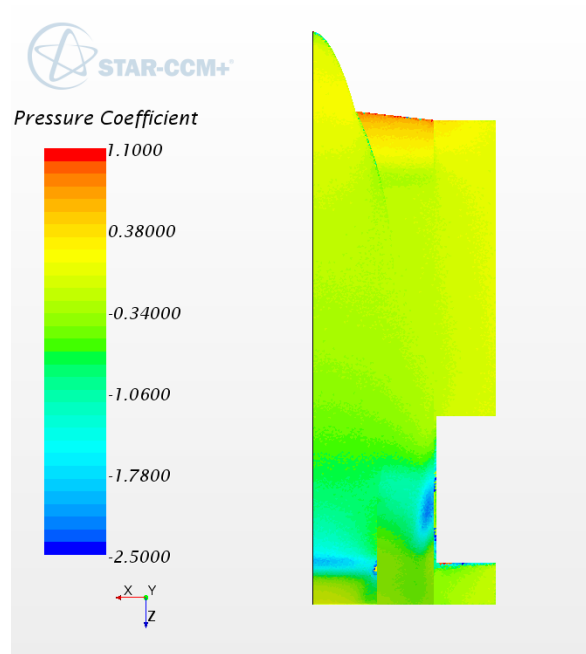


Figure 29:  $C_p$  for under-tray Double Diffusers

## 3.7 3-D Gurney Flap Study

### 3.7.1 Overview

A gurney is a non Bernoulli device which operates by increasing the pressure on the pressure side of the wing and decreasing the pressure on the suction side of the wing. At the same time it helps in keeping the flow attached all the way till the trailing edge. A gurney flap on the diffuser will

aid by reducing the pressure on the suction side of the diffuser. The efficiency of the gurney flap is dependent on the aerodynamic flow design of the entire body. Here we are looking at free stream results for the best possible design. The use of gurney flap is to maximize the down-force producing potential of the entire package. The gurney flap study was performed on a double diffuser under-tray with angles of 26 degrees on both of them. Different sizes of gurney were tested for down-force or  $C_L$  numbers. The following column show the results

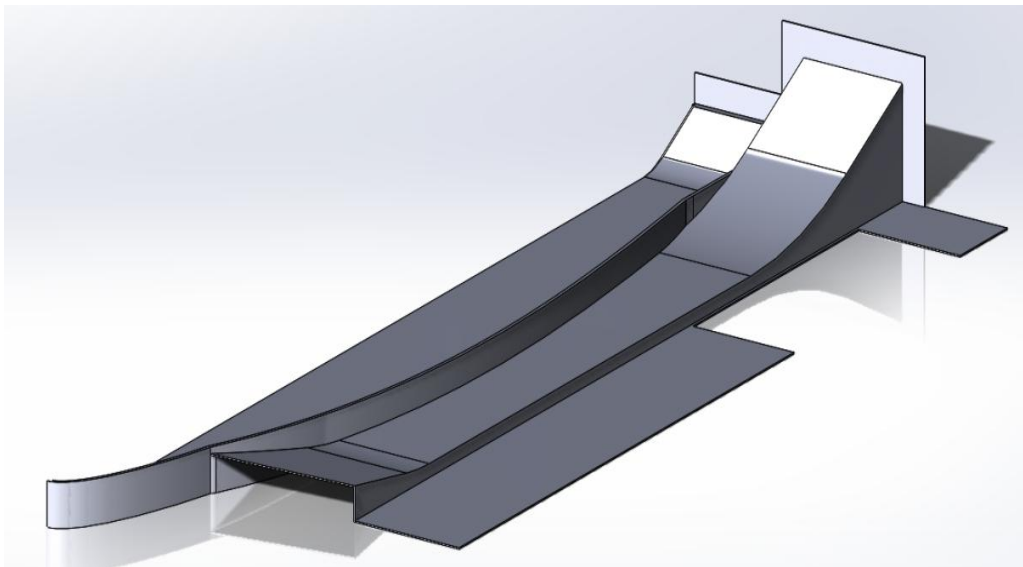


Figure 30: Solid works model of double diffuser under-tray with gurney

### 3.7.2 Result

Various sized gurney flaps were tested as can be seen below in Table-3.

The addition of gurney flap increased the  $C_i$  by around 15%. For manufacturing reasons the gurney flap selected was 2in. Since the gains above that are negligible.

Table 3: Gurney flap study for under-tray with double diffuser

Length	$C_i$
0.5	0.38
1	0.42
1.5	0.44
2	0.47
2.5	0.48

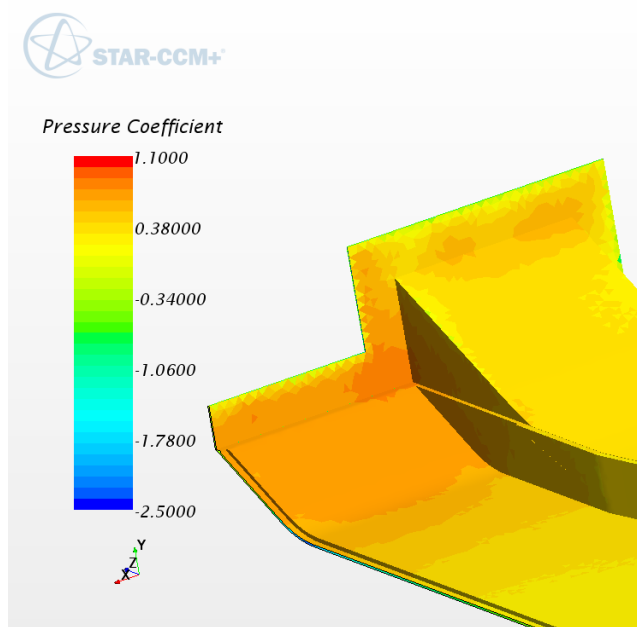


Figure 31 : Pressure Coefficient plot for double diffuser with gurney flap

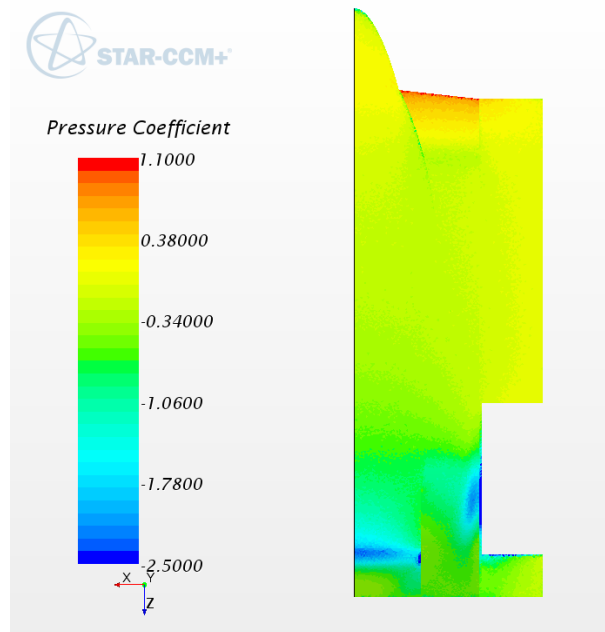


Figure 32: Pressure Coefficient plot for double diffusers with gurney flap

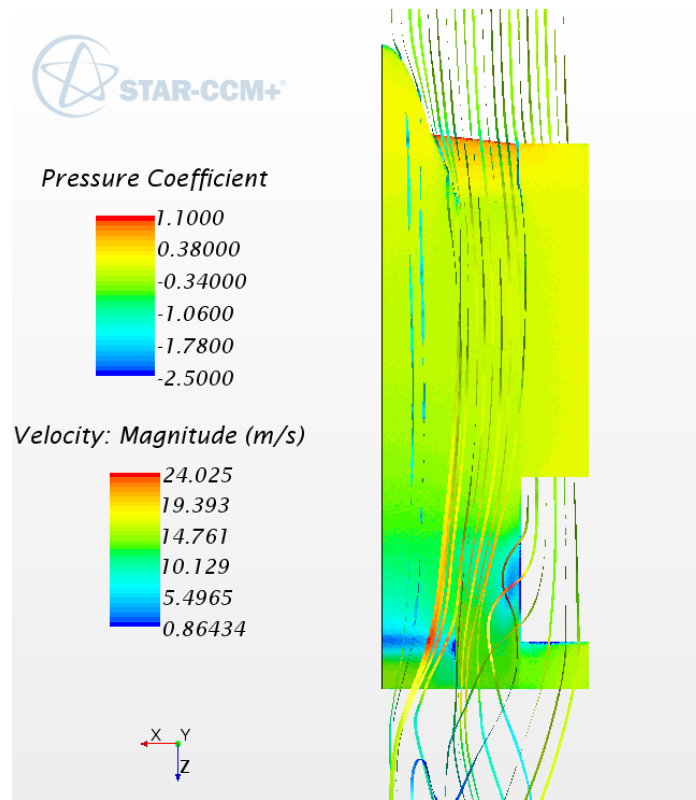


Figure 33 : Velocity stream lines for double diffusers with gurney flap

### 3.8 3-D Analysis Of Final Model

For the final model all the parameters were selected from previous results. The inlet angle used was 9 degree, with a inlet area ratio of about 1.9. The angles for both diffusers are 26 degree and a gurney flap of 2in is used. For the final study we used half the under-tray with a symmetric wall and mirrored the final results. The CFD software Star Ccm+ helps us to simulate the other of the symmetric after the simulation has converged. All the below figures and pictures are from Star Ccm+. Two configuration of

simulations were run to understand the effects of a static and rotating tire on the under-tray. The figures and pressure plots are as below.

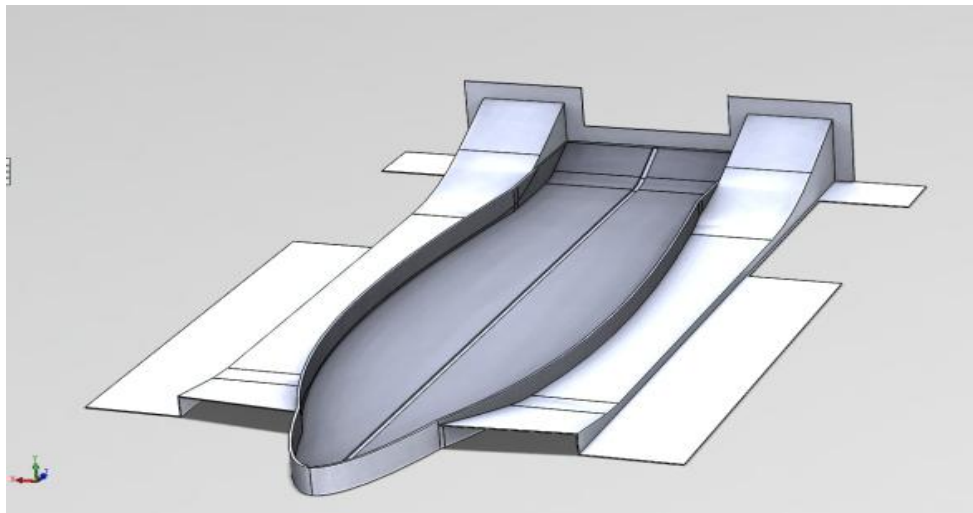


Figure 34 : Solid works full under-tray model

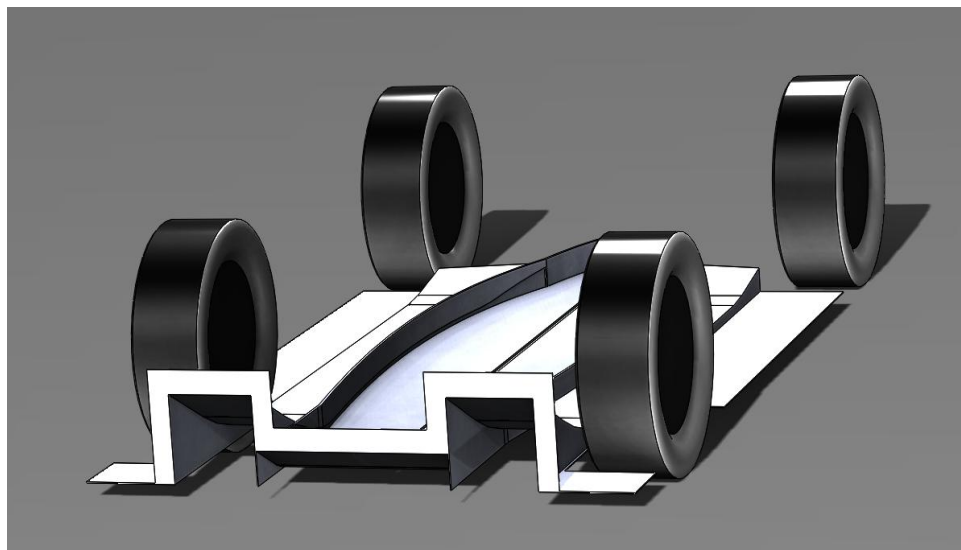


Figure 35: Solid works full under-tray model with tires

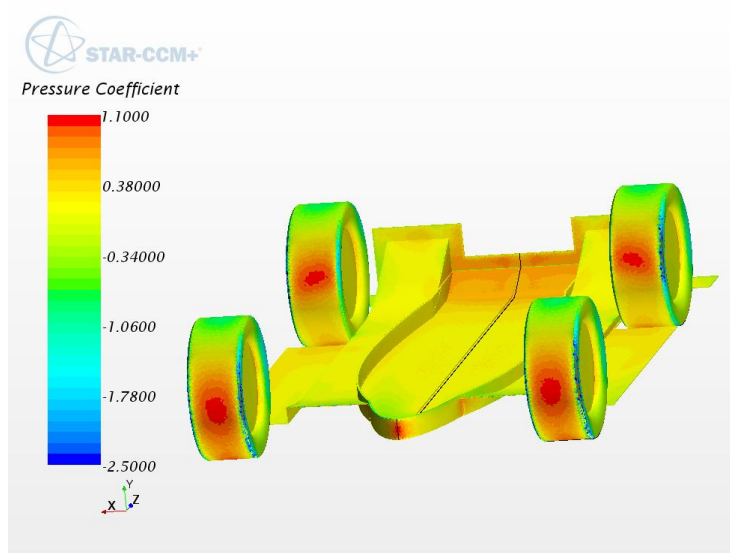


Figure 36 : Pressure Coefficient plot for under-tray with tires-1

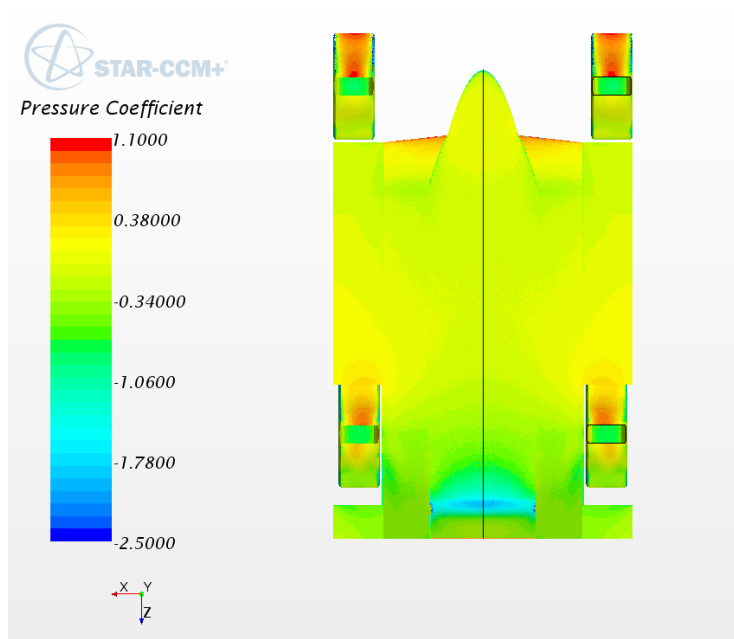


Figure 37: Pressure Coefficient plot for under-tray with tires-2

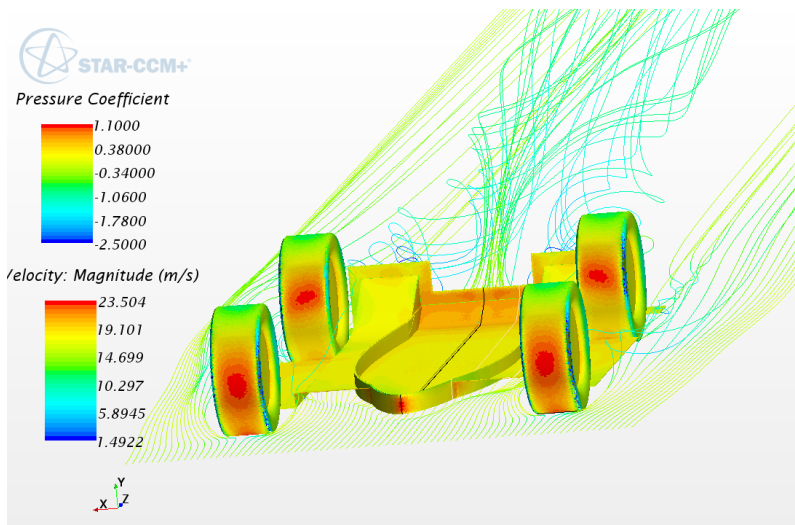


Figure 38 : Velocity streamlines for Under-tray with tires

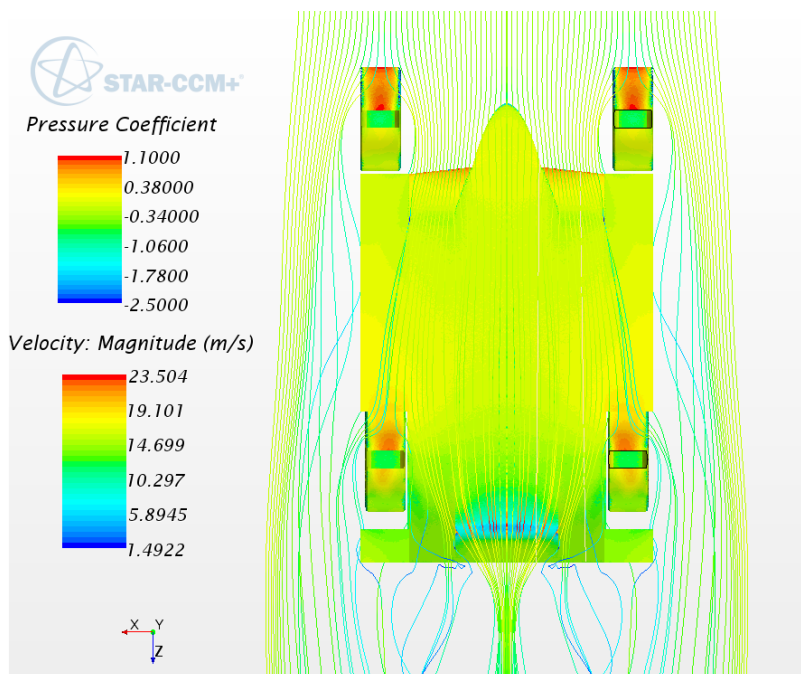


Figure 39: Velocity stream lines for double diffusers with gurney flap



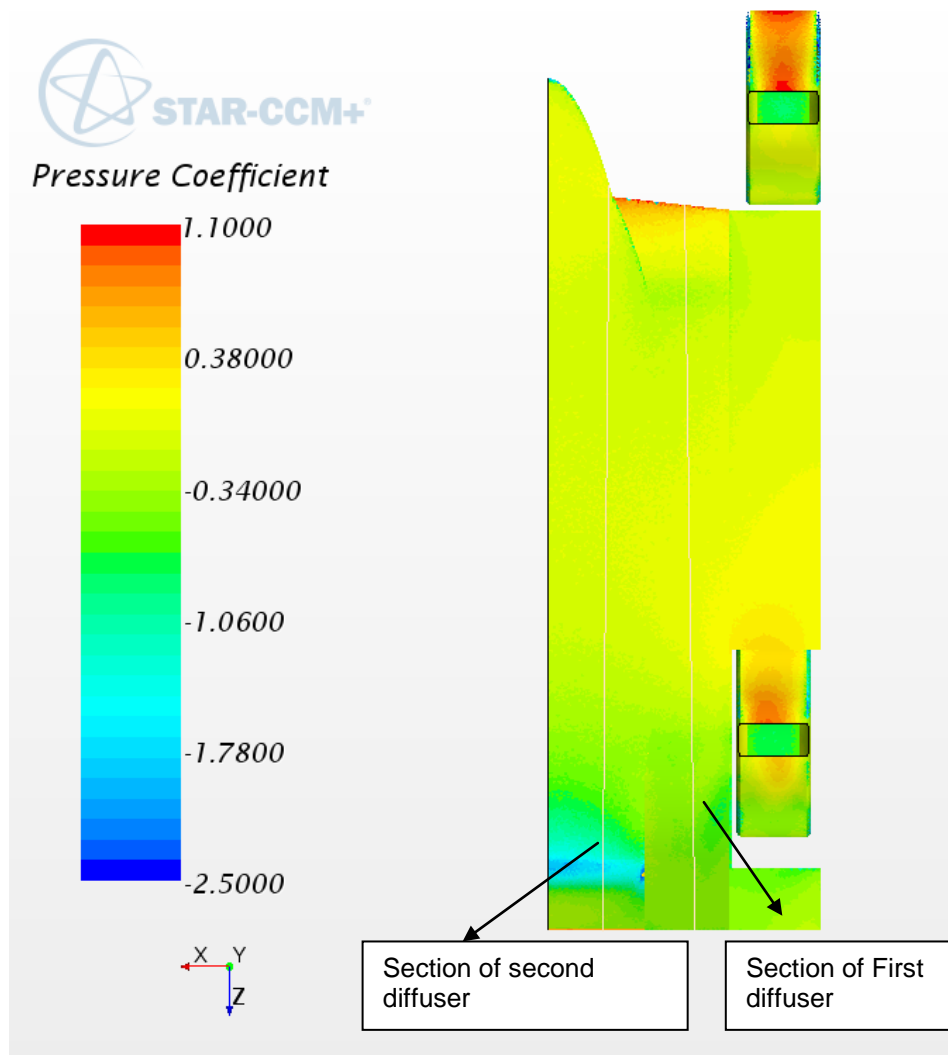


Figure 40: Pressure curves from inlet to diffuser outlet

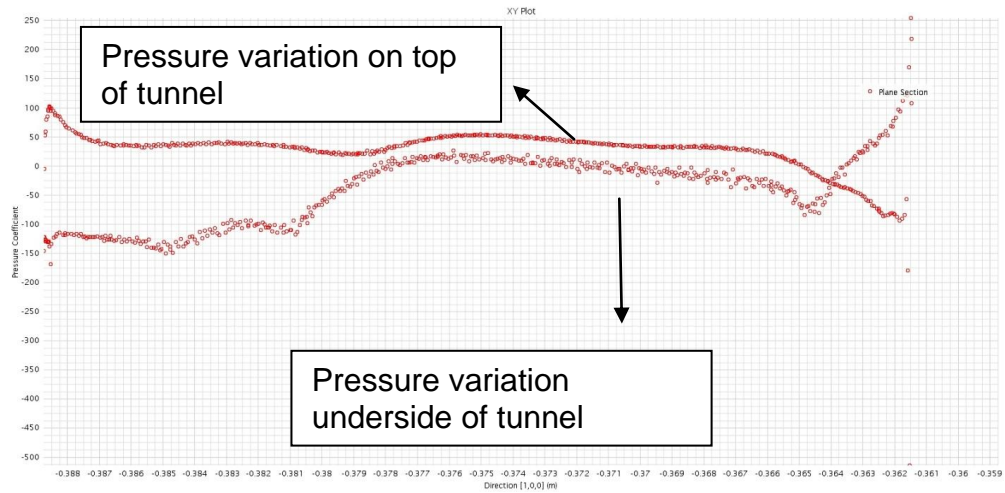


Figure 41: Pressure Coefficient vs Length of under-tray (First Diffuser)

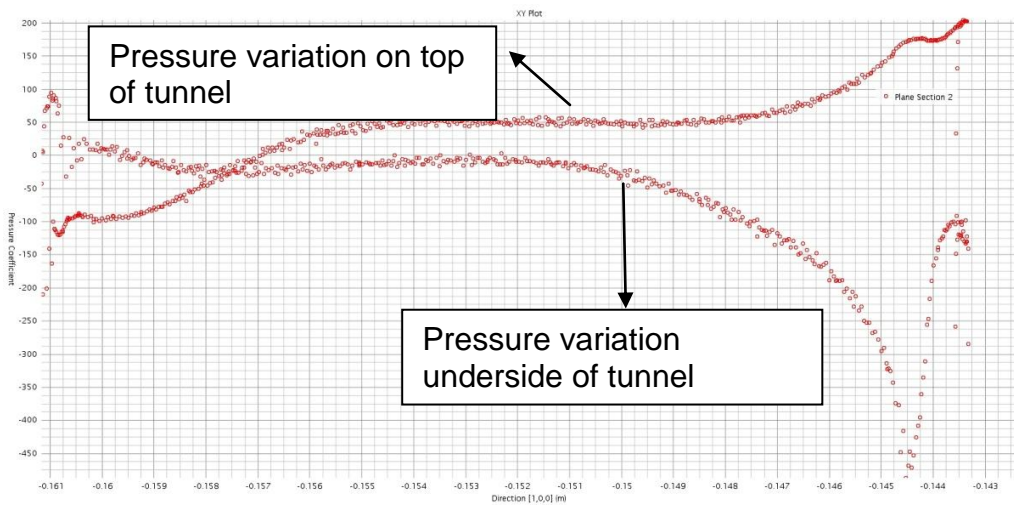


Figure 42: Pressure Coefficient vs Length of under-tray (Second Diffuser)

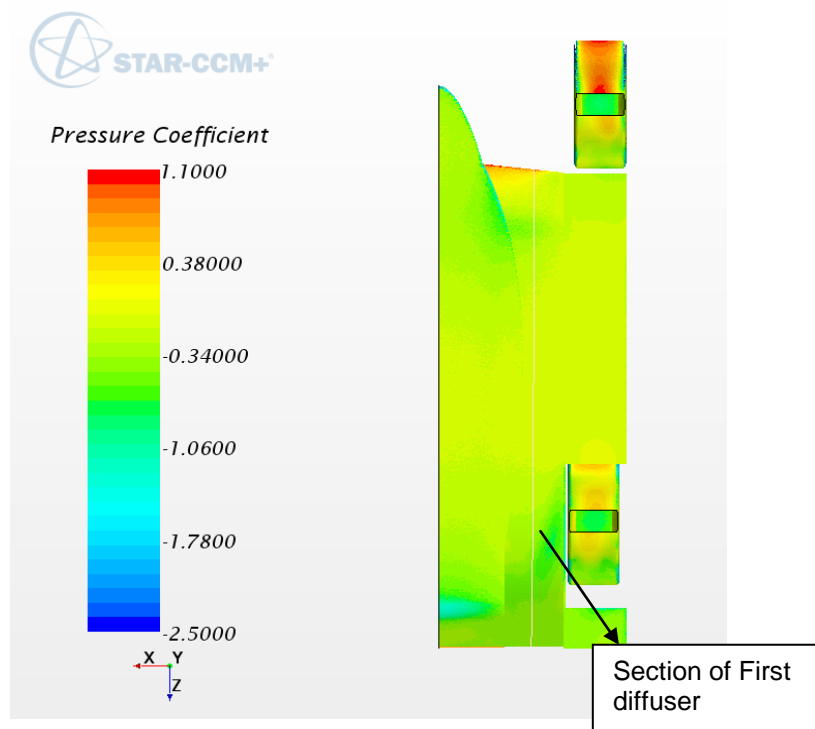


Figure 43 : Pressure coefficient plot of Under-tray With 2-Degree Pitch

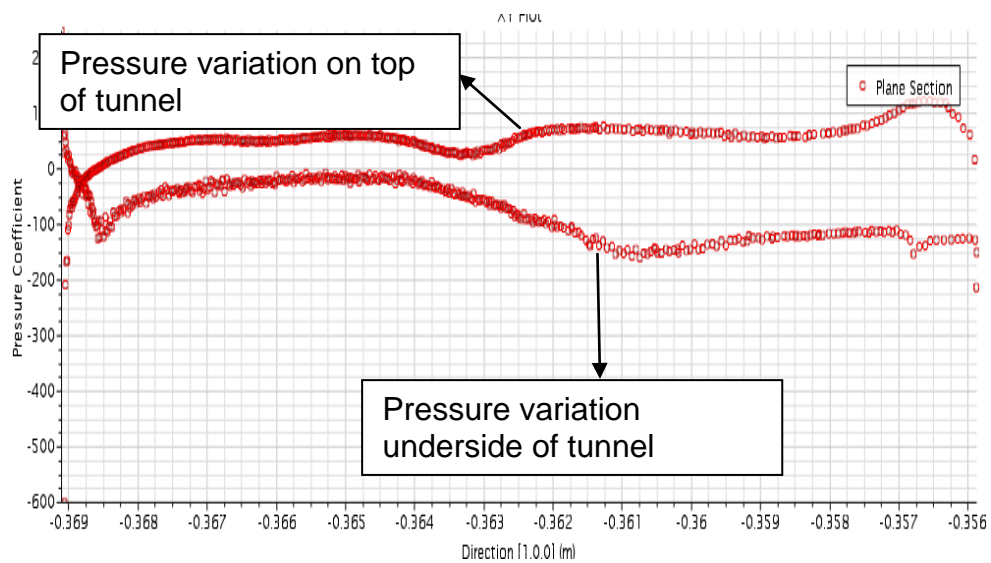


Figure 44: Pressure Coefficient vs Length of under-tray

### 3.8.1 Results

The addition of second diffuser and gurney flap increased the  $C_l$  by 23% from the base straight tunnel model.

The conclusion of the 3-D analysis is that we were able to increase the down-force of the new under-tray by 33% compared to the old diffuser design in free stream. Addition of the gurney flap increased it by 50% more. As said in the beginning the idea was to design an under-tray which has the maximum potential to produce down-force. Which has been achieved. Table 4 has the final results of various under-trays modeled at 30m/s or 67 mph.'

Table 4: Final results of 3-D analysis

<b>Under tray type</b>	<b>Down-force(LBF)</b>
Old under-tray free stream (2006)	93
Under-tray w/o gurney	120
Under-tray with gurney	146
Under-tray w/o gurney rotating tires	73
Under-tray with gurney rotating tires	84
Under-tray in 2 degree pitch	115

### 3.9 Ride Height Study

Ride Height has a effect on the performance of the under-tray. As mentioned in the previous section, the baseline under tray at 1.75 inch of ride height produced 146 LBF of down force. That same under tray at a ride height of 1.5 of 140 LBF and at 1 inches produced 132 LBF of down force. This equates to a 10% drop in down force by the ride height of the under tray a mere 0.75 inches or 19mm. Figure shows the impact of ride height on the  $C_p$  of the under tray.

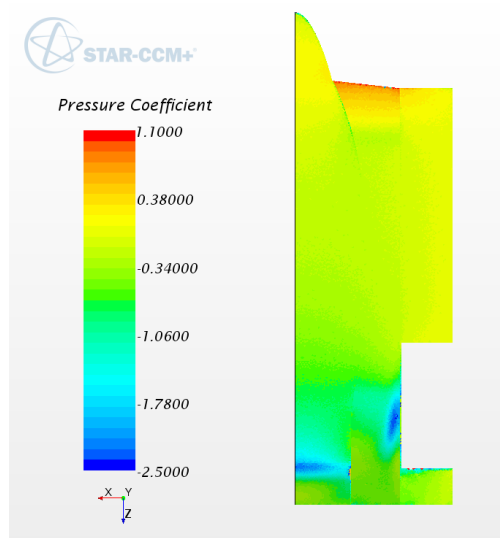


Figure 45: Pressure Coefficient at 1.5in ride height

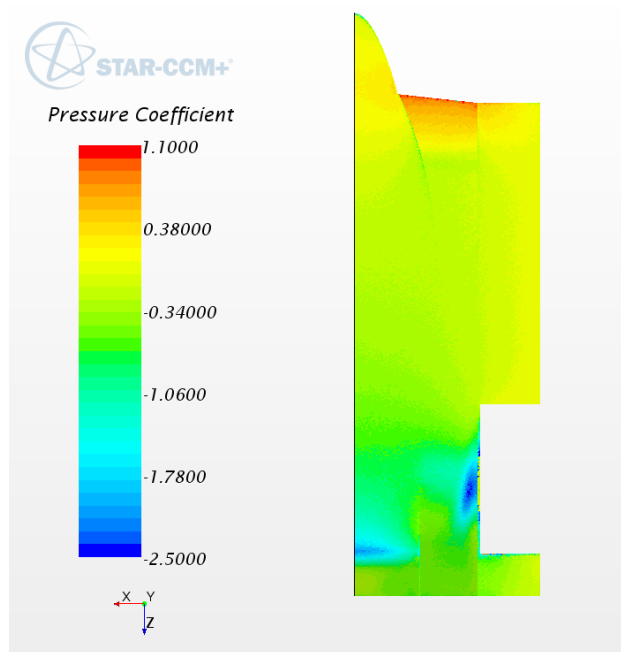


Figure 46:Figure 45:Pressure Coefficient at 1in ride height

### 3.10 Recommendations

Create a CFD model of the full car with chassis, front and rear wing and suspension arms at the 1.75" ride height with rotating tires to see how the surrounding components effect the down force the under tray generates.

Take the completed under-tray to a wind tunnel this fall to evaluate the under-tray and correlate the down-force and drag numbers with the wind tunnel values.

Run a cruise test with a new under-tray on an Formula car. Get shock pot data from the suspension system to correlate the CFD values with the actual numbers

## References

- (1) Katz, Joseph. Race Car Aerodynamics. Cambridge:2005
- (2) Elliott, Aaron. Formula SAE Vehicle Aerodynamics: Under-tray Optimization Study:2006



## Biographical Information

Girish Bangalore Jalappa was born in Bangalore, India on August 21st 1987. He completed his Bachelors in Mechanical engineering from Dayananda Sagar College Of Engineering, India in Dec 2011.

He began his graduate studies at University of Texas at Arlington. To pursue his research interest in Fluid dynamics(Aerodynamics) he joined the UTA FSAE team and worked under Dr. Robert L Woods . His research work during the graduate course involved designing aerodynamics package for the FSAE race car and worked as the aerodynamics lead for the year 2014-15. He plans to pursue his interests in race car aerodynamics by taking up related projects in the industry and all allied fields.